MECHANICAL PROPERTIES OF HIGH ENTROPY ALLOY TiC REINFORCED IN-SITU COMPOSITE

Igor MORAVČÍK, Jan ČÍŽEK, Ivo DLOUHÝ

Institute of Materials Science and Engineering - NETME Centre, Faculty of Mechanical Engineering, Brno University of Technology (BUT), Brno, Czech Republic, EU, moravciktk@gmail.com

Abstract

The present work is focused on the synthesis of inequiatomic AlCoCrFeNiTi$_{0.5}$ high entropy alloy (HEA) with composite structure reinforced by TiC nanoparticles. The initial alloy was prepared by mechanical alloying (MA) in a planetary ball mill, compacted by spark plasma sintering (SPS) and heat treated to obtain better microstructure. Microstructure and mechanical behavior of the SPS-ed compacts prior to and after the heat treatment were investigated. The bulk samples were composed of nano-grained mixture of FCC solid solution, ordered BCC phase and in-situ formed TiC nanoparticles. The high hardness of 803 HV and 564 HV of the alloy in SPS-ed and heat treated state was measured with bending strength of the latter reaching a value of 2 GPa. It was shown that a fabrication of TiC reinforced HEA nanocomposites with excellent mechanical properties can be achieved.

Keywords: High entropy alloy, powder metallurgy, sintering

1. INTRODUCTION

Conventionally, the alloy design, production, and selection are almost strictly confined to single element based concept where the properties are adjusted by relatively small additions of different elements [1]. Consequently, this alloy concept imposes a significant limit to the degrees of freedom in the alloy's composition and thus limits the development of special microstructure and properties. In the last decade, such alloying concept has been overcome due to an appearance of new class of alloys, named high entropy alloys (HEA) [2] as the high configurational entropy was initially believed to stabilize their solid solution microstructures. These alloys do not contain a single base element, but rather multiple principal elements, usually over 5, with near equiatomic proportions. The combination of mostly simple solid solution microstructures (either FCC or BCC) and inherent extreme substitutional solid solution strengthening effect [3] gave rise to a combination of exceptional properties such as wear and corrosion resistance [4, 5], high mechanical strength and ductility [6, 7], high temperature strength [8] etc. HEA can be also conveniently used as matrix phase for metal matrix composites (MMC) with high mechanical properties [9-11]. As opposed to traditional casting manufacturing route, powder metallurgy route (PM) is an alternative way for production of HEA and other complex materials, exploiting the advantage of lower processing temperatures, thus avoiding casting segregations and inhomogeneity's in the final product [12, 13]. For the PM preparation of HEA, mostly mechanical alloying of elemental powders with subsequent spark plasma sintering (SPS) is used due to its simplicity and relatively short processing times [14, 15]. A full density of bulk samples is achieved relatively rapidly, which enables for the production of bulk materials and MMC with nano-scale grains [14, 15]. In the presented study, in-situ TiC reinforced HEA MMC with AlCoCrFeNiTi$_{0.5}$ chemical composition chosen for a good combination of properties [1, 16] has been manufactured.

2. EXPERIMENTAL

AlCoCrFeNiTi$_{0.5}$ (in atomic proportion) HEA powders were prepared by high-energy ball milling process in a planetary ball mill. For the milling, commercial purity Al, Cr, Co, Fe, Ni, Ti, and elemental powders with the average particle sizes around 45 μm were utilized. The powders were sealed in a steel milling bowl with the

ball to powder weight ratio (BPR) of 10:1. Methanol was used as the process control agent (PCA) to prevent powder agglomeration during milling. The milling conditions of 24 hours milling time with 400 RPM were obtained from preliminary optimization studies. The final processed powders were further consolidated by SPS (Thermal Technology LSS 10-4) in a 30 mm graphite die at Institute of Plasma Physics of Czech Academy of Sciences. Graphite foils were placed between the powders and the die walls to prevent mutual fusing. A sintering temperature of 1100 °C with 60 MPa pressure and 8 minutes holding time were used for the consolidation. After SPS, heat treatment of the samples was carried out at 1250 °C followed by air cooling to invoke prospective changes in the structure (grain size unification and porosity reduction). A tube furnace Carbolite Gero STF with protective argon gas atmosphere has been used for the heat treatment experiments. The final samples were 6 mm high cylinders with 30 mm diameter. XRD technique with Philips X´Pert, 40 kV, Co Kα radiation at λ = 0.17903 nm, 2θ = 30-120° was used to observe the phase composition after the different processing steps. Samples for microstructural observation were prepared by standard metallographic procedures. Polished samples were analyzed by ZEISS Ultra Plus SEM at an accelerating voltage of 20 kV and 10 kV followed by energy dispersive microanalysis method (EDS). Hardness measurement was carried out using Vickers microhardness tester with 200 g work load on polished samples. Porosity was measured by image analysis with ImageJ software on the polished samples. The room temperature bending strength (R_{mb}) was measured using three-point bending jig on Zwick Z020 universal tensile test machine, with the loading span of 18 mm and a crosshead speed of 1 mm·min^{-1}. The samples had nominal dimensions of 22 × 6 × 4 mm and were manufactured from the SPS-ed cylinder using wire electric discharge cutting.

3. RESULT AND DISCUSSION

3.1. XRD phase analysis

The XRD pattern of the AlCoCrFeNiTi$_{0.5}$ powders milled with 15 mm balls under 400 RPM for 24 hours is presented in **Figure 1a**. The powders are composed of a single BCC solid solution that was formed from the elemental powders due to mechanical alloying process. The observed peak broadening points out to a significant grain refinement. The patterns of the SPS-ed bulk produced from these powders is presented along with the bulk alloy after heat treatment at 1250 ºC in **Figures 1b** and **1c**, respectively. The as-SPS-ed material and after the HT at 1250 ºC are composed of the same phases, i.e. FCC Fe- and Cr-enriched solid solutions, a B2 ordered phase enriched in Ni and Al and in-situ formed TiC. The appearance of the TiC phase is very interesting, especially considering that no intentional addition of carbon to the powders was made. Its presence is attributed to the addition of methanol (CH_3OH) to the powders as a PCA. During the milling process, methanol was most likely trapped between the powder particles that were cold welded together. Subsequently, it decomposed and dissolved into the lattices of the powders. After the sintering, the high affinity of carbon to titanium resulted in the formation of the TiC phase. The calculated volume fraction of the present phases (from XRD patterns) is 26.5% FCC phase, 58% B2 phase, and 15.5% TiC.

3.2. Microstructure analysis

The microstructure of SPS-ed sample and heat treated sample as evaluated by SEM microstructural observations is presented in **Figure 2**. According to the EDS chemical analysis, the phase composition remained unchanged after the HT procedure and closely matches the desired composition (not shown due to limited space). The observed phase composition is in good agreement with XRD results from **Figure 1**. It seems that the remains of original powder particles are still distinguishable in the microstructure after SPS (for better clarity denoted by red circles in **Figure 1a**), with very fine FCC, B2 and TiC phase mixtures. These “islands” are surrounded by much coarser, brighter FCC phase. The microstructure seems rather homogenous, with few pores present (overall porosity measured to be below 0.5%). The microstructure after the HT procedure is coarsened; however, the remnants of the original particle boundaries are still visible. The

TiC phase particles inside the original ”islands” have slightly coarsened to the size of hundreds of nanometers. Their dispersion is very homogenous while they possess essentially favourable, globular morphology.

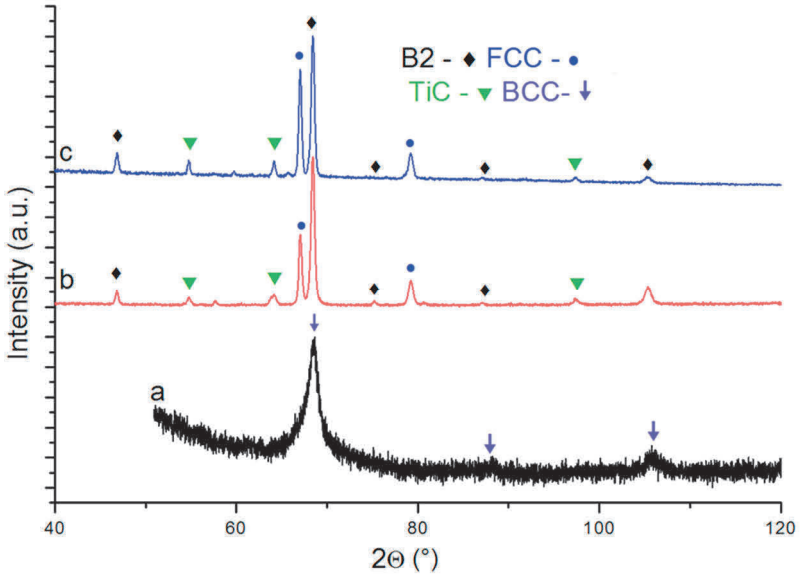

Figure 1 XRD pattern of AlCoCrFeNiTi0.5 a) powder milled with 400 RPM, 24h and 15 mm balls; b) SPS-ed bulk alloy B c) SPS-ed alloy B after heat treatment at 1250 ºC

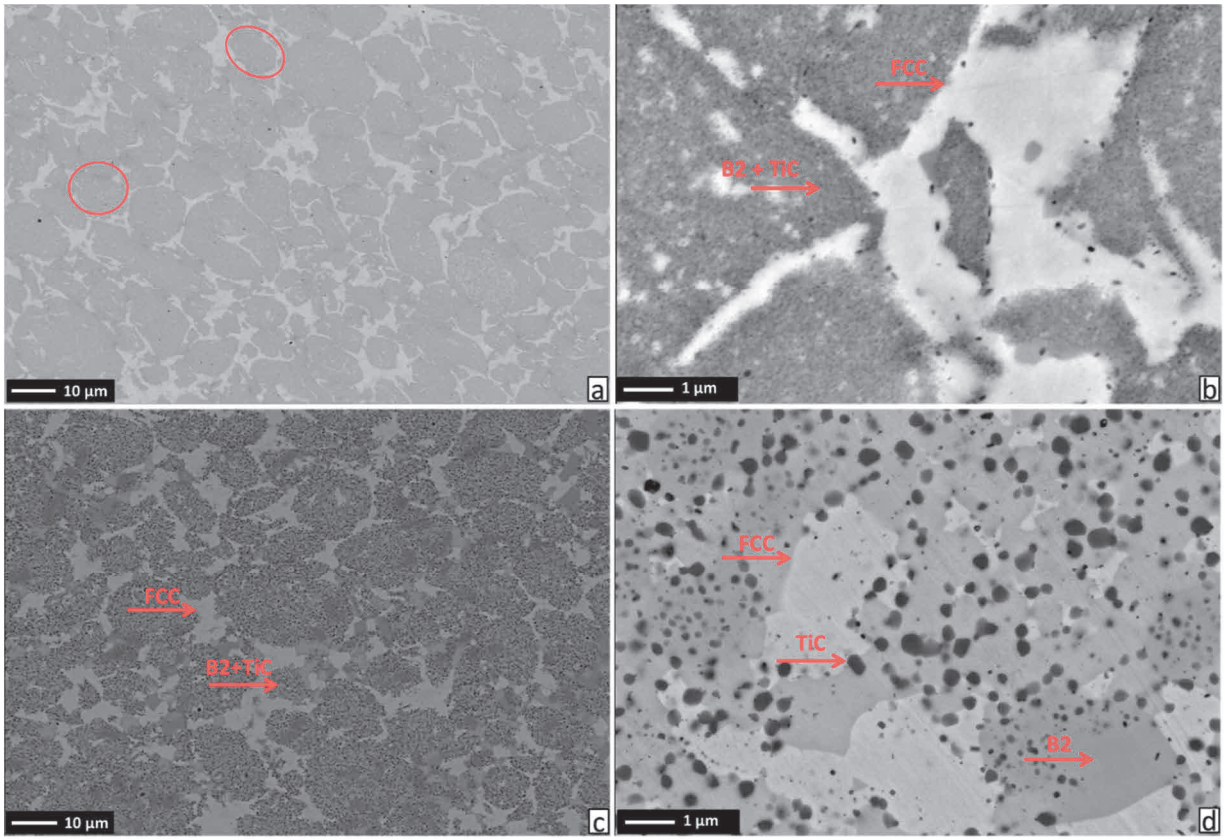

Figure 2 SEM micrographs in back scattered mode (BSE) with marked phases of AlCoCrFeNi$Ti_{0.5}$ bulk alloy microstructure; a) b) after SPS densification, c) d) after heat treatment at 1250 ºC

3.3. Mechanical testing

The measured hardness of the alloy after SPS was 803 ± 40 HV0.2 (presented in **Table 1**) - a very high value attributed to the combination of Orowan strengthening from TiC dispersion and the very fine grain sizes. The heat treatment at 1250 ºC caused hardness decrease to 564 ± 33 HV0.2 as a consequence of the grain coarsening. The results obtained from bending testing of SPS-ed + heat treated samples are presented in **Table 1**. The bending strength of the SPS-ed sample was not measured, due to limited available material [17]. The measured bending strength of the material was significantly high, reaching almost 2 GPa, with relatively low scatter. This may be ascribed to a very homogenous microstructure. However, a brittle fracture has been observed upon rupture, with no significant plastic deformation preceding the fracture.

Table 1 Results of three-point bending test of $AlCoCrFeNiTi_{0.5}$ bulk after SPS and heat treatment.

Sample	R_{mb} (MPa)	E (GPa)	Max. deflection (mm)
SPS + HT 1250 ºC	**1992** ± 164	99.4	0.4 ± 0.2

Figures 3a, b and **c** denotes the fractured surfaces of the broken bending specimen of the SPS-ed alloy, heat treated at 1250 ºC. The initiation site of the fracture was probably a surface defect from which the fracture rapidly propagated throughout the specimen cross - section. The specimen was cracked in a brittle fracture manner. Transgranular fracture features with visible cleavage facets (denoted by yellow arrow) are visible. In some places on fracture surface (**Figure 3c**), the areas with brittle fracture are surrounded by ductile dimples (marked by green arrow).

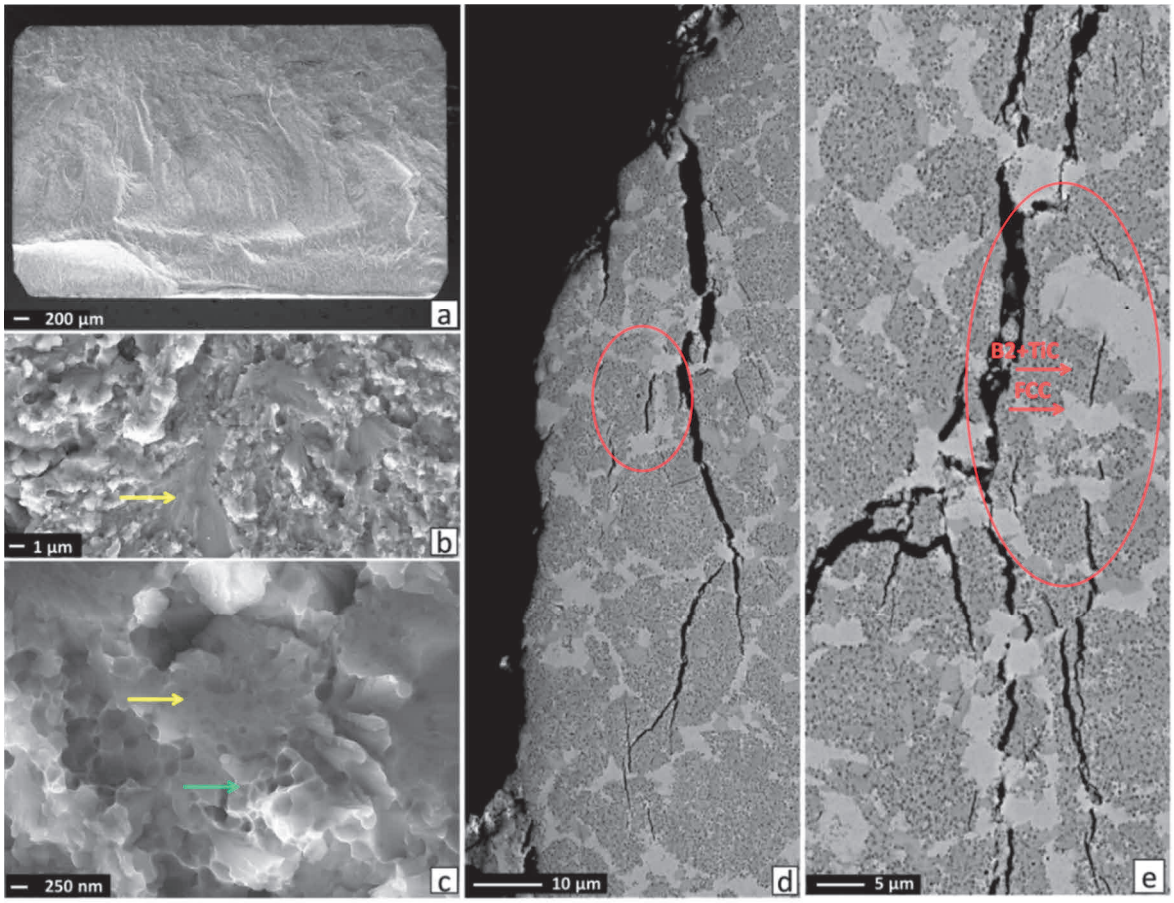

Figure 3 SEM micrographs of bulk alloy a, b, c) fracture surfaces of SPS-ed and 1250 °C heat treated bend test specimens; d,e) side view of polished fractured specimen revealing the crack propagation mechanism

This arrangement of the fracture morphology well corresponds to the hard “islands” of B2/TiC phase mixture surrounded by the intrinsically ductile FCC phase, observed in the SEM imaging. SEM micrographs taken from a polished bending specimen side (in direction perpendicular to fracture surface) are presented in **Figures 3d** and **e**. Secondary cracks located near the magistral crack below the fracture surface are observed. The cracks growth occurs preferentially in the regions of B2/TiC phase mixture that are seemingly very brittle in nature (denoted by red arrow and red ellipse of **Figure 3d**). While the B2/TiC islands are already cracked, the ductile FCC phase grains are being plastically deformed, causing the crack bridging phenomenon. In this fashion, FCC grains are retarding the propagating cracks, causing the extrinsic toughening effect in the material. This ductile phase crack bridging may be one of the reasons for the extraordinary high values of the bending strength of this composite.

4. CONCLUSIONS

In the presented work, high entropy alloy MMC with fine dispersion of TiC reinforcement has been produced by a combination of reactive milling and spark plasma sintering. The conclusions are drawn as follows:

- $AlCoCrFeNiTi_{0.5}$ alloy can be efficiently produced by PM processes possessing high hardness and full density microstructure;
- The use of carbon containing process control agent resulted in the in-situ formation of TiC dispersion after SPS densification of $AlCoCrFeNiTi_{0.5}$ alloy;
- Subsequent heat treatment at 1250 °C resulted in a slight grain coarsening and a corresponding drop in hardness;
- Very high bending strength value reaching up to 2 GPa has been measured in the heat treated state with crack bridging mechanism by ductile FCC phase during the bulk alloy fracture.

ACKNOWLEDGEMENTS

The research was funded by the Ministry of Education, Youth and Sports within the „National Sustainability Programme I“ (NETME CENTRE PLUS - LO1202). The results were obtained within the PhD thesis of the author [17]. Authors would also like to thank Dr. Radek Musalek from Institute of Plasma Physics of Czech Academy of Sciences in Prague for SPS consolidation experiments.

REFERENCES

[1] MIRACLE, D.B. and SENKOV, O.N. A critical review of high entropy alloys and related concepts. Acta Mater. 2017. vol. 122, pp. 448-511. doi:https://doi.org/10.1016/j.actamat.2016.08.081.

[2] PICKERING, E.J. and JONES, N.G. High-entropy alloys: a critical assessment of their founding principles and future prospects. I*nt. Mater. Rev*. 2016. vol. 61, pp. 183-202. doi:10.1080/09506608.2016.1180020.

[3] WU, Z., TROPAREVSKY, M.C., GAO, Y.F., MORRIS, J.R. STOCKS, G.M. and BEI, H. Phase stability, physical properties and strengthening mechanisms of concentrated solid solution alloys. *Solid State Mater. Sci*. 2017, vol. 21, pp. 267-284. doi:https://doi.org/10.1016/j.cossms.2017.07.001.

[4] WU, J.-M., LIN, S.-J., YEH, J.-W., CHEN, S.-K., HUANG, Y.-S. and CHEN, H.-C. Adhesive wear behavior of AlxCoCrCuFeNi high-entropy alloys as a function of aluminum content. *Wear*. 2006, vol. 261, pp. 513-519. doi:http://dx.doi.org/10.1016/j.wear.2005.12.008.

[5] HUANG, P.K., YEH, J.W., SHUN, T.T. and CHEN, S.K. Multi-principal-element alloys with improved oxidation and wear resistance for thermal spray coating. *Adv. Eng. Mater*. 2004. no. 6, pp. 74-78. doi:10.1002/adem.200300507.

[6] LI, Z., KÖRMANN, F., GRABOWSKI, B. NEUGEBAUER, J. and Raabe, D. Ab initio assisted design of quinary dual-phase high-entropy alloys with transformation-induced plasticity. *Acta Mater*. 2017, vol. 136, pp. 262-270. doi:http://dx.doi.org/10.1016/j.actamat.2017.07.023.

[7] ZHANG, Z., SHENG, H., WANG, Z. GLUDOVATZ, B., ZHANG, Z. and GEORGE, E.P. Dislocation mechanisms and 3D twin architectures generate exceptional strength-ductility-toughness combination in CrCoNi medium-entropy alloy. *Nat. Commun*. 2017, no. 8, p. 14390. doi:10.1038/ncomms14390.

[8] SENKOV, O.N., WILKS, G.B. SCOTT, J.M. and MIRACLE, D.B.Mechanical properties of Nb25Mo25Ta25W25 and V20Nb20Mo20Ta20W20 refractory high entropy alloys. *Intermetallics*. 2011. vol. 19, pp. 698-706. doi:http://dx.doi.org/10.1016/j.intermet.2011.01.004.

[9] MORAVCIK, I., GOUVEA, L., CUPERA, J. and DLOUHY, I.Preparation and properties of medium entropy CoCrNi/boride metal matrix composite. *J. Alloys Compd*. 2018. no. 748. doi:10.1016/j.jallcom.2018.03.204.

[10] MORAVCIK, I., CIZEK, J., GAVENDOVA, P., SHEIKH, S., GUO, S. and DLOUHY, I. Effect of heat treatment on microstructure and mechanical properties of spark plasma sintered AlCoCrFeNiTi0.5 high entropy alloy. *Mater. Lett*. 2016. no. 174. doi:10.1016/j.matlet.2016.03.077.

[11] HADRABA, H., CHLUP, Z., DLOUHY, A., DOBES, F., ROUPCOVA, P., VILEMOVA, M. et al. Oxide dispersion strengthened CoCrFeNiMn high-entropy alloy. *Mater. Sci. Eng. A*. 2017. vol. 689, pp. 252-256. doi:http://dx.doi.org/10.1016/j.msea.2017.02.068.

[12] GERMAN, R.M. *Powder Metallurgy Science*. 2nd ed., Princeton MPIF, Princeton, 1994.

[13] MORAVCIK, I., CIZEK, J., ZAPLETAL, J., KOVACOVA, Z., VESELY, J., MINARIK, P.et al. Microstructure and mechanical properties of NiCoCrFeTi high entropy alloy fabricated by mechanical alloying and spark plasma sintering. *Mater. Design*. 2017, vol. 119. doi:10.1016/j.matdes.2017.01.036.

[14] ROGAL, Ł., KALITA, D., TARASEK, A., BOBROWSKI, P. and CZERWINSKI, F. Effect of SiC nano-particles on microstructure and mechanical properties of the CoCrFeMnNi high entropy alloy. *J. Alloys Compd*. 2017. vol. 708, pp. 344-352. doi:http://doi.org/10.1016/j.jallcom.2017.02.274.

[15] FU, Z., MACDONALD, B.E., ZHANG, D., WU, B., CHEN, W., IVANISENKO, J. et al., Fcc nanostructured TiFeCoNi alloy with multi-scale grains and enhanced plasticity. *Scr. Mater*. 2018. vol. 143, pp. 108-112. doi:https://doi.org/10.1016/j.scriptamat.2017.09.023.

[16] ZHANG, K.B., FU, Z.Y., ZHANG, J.Y., WANG, W.M., WANG, H., WANG, Y.C. et al. Microstructure and mechanical properties of CoCrFeNiTiAlx high-entropy alloys. *Mater. Sci. Eng. A*. 2009. vol. 508, pp. 214-219. doi:10.1016/J.MSEA.2008.12.053.

[17] Moravcik, I. *Metal matrix composites prepared by powder metallurgy route*. PhD thesis. Brno: University of Technology. 2017. 149 p. https://www.vutbr.cz/www_base/zav_prace_soubor_verejne.php?file_id=160762.